Antimony Oxybromide/Graphitic Carbon Nitride Composites: Synthesis, Characterization, Degraded Mechanisms, and Photocatalytic Activity of CO_2 Reduction and CV Degradation

國立台中教育大學 科學教育與應用學系
大四專題生 翟振廷
指導教授 陳錦章 講座教授兼理學院院長

Abstract

In this study, $Sb_4O_5Br_2$ was prepared by high-pressure hydrothermal method with $SbBr_3$ and H_2O. A variety of photocatalysts and the best catalyst composite graphitic carbonitride (g-C_3N_4) were synthesized by changing the temperature and time. Various instruments such as XRD, DRS, FT-IR, SEM-EDS, FE-TEM-EDS, HP-XPS, BET, and PL were used to determine the composition, physical and chemical properties, band gap, and compound structure of the photocatalyst. Its activity was evaluated by the reduction of CO_2 to organic compounds, such as CH_4, and the photocatalytic degradation of crystal violet (CV) dyes. The photocatalytic activity of $Sb_4O_5Br_2$/g-C_3N_4 was significantly improved compared with bare $Sb_4O_5Br_2$ and g-C_3N_4. $Sb_4O_5Br_2$/g-C_3N_4-75wt% possessed the highest rate constant of 0.0328 h^{-1} for the degradation of crystal violet (CV), which was nearly 4.2 and 1.1 times higher than that of $Sb_4O_5Br_2$ and g-C_3N_4. GC was used to analyze the efficiency of CO_2 reduction under visible light irradiation. The results provided a critical advance in photocatalytic conversions of CO_2 into C_{2+} compounds, such as C_nH_{2n+2}, C_nH_{2n}, and C_nH_{2n-2} ($n < 6$), which played essential roles in the current chemical or energy industry. Therefore, the findings of this study will contribute to the understanding of CO_2 activation in photocatalytic reduction and highly selective production of hydrocarbons through C-C coupling reactions.

Results and Discussion

XRD

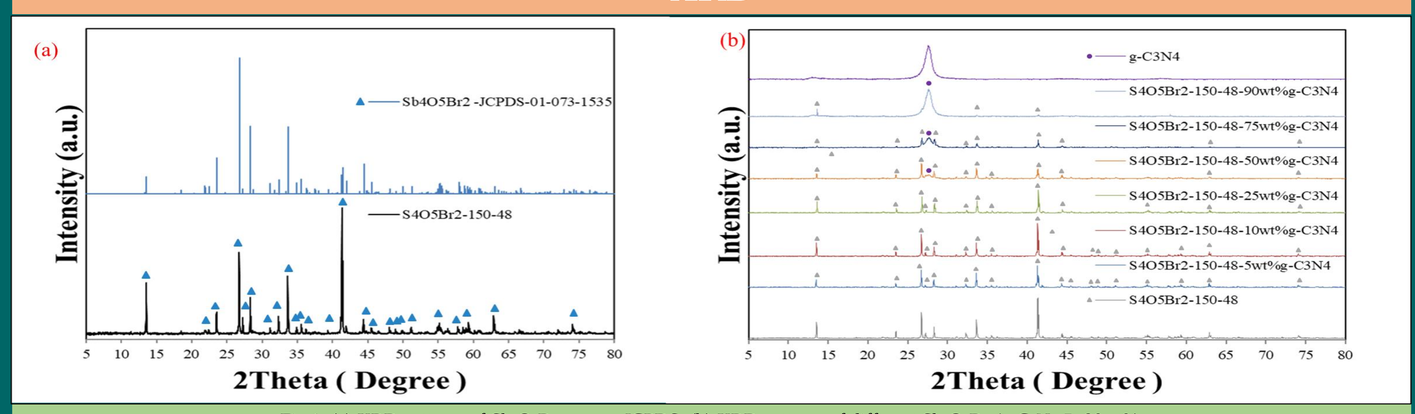

Fig 1. (a) XRD patterns of $Sb_4O_5Br_2$ versus JCPDS, (b) XRD patterns of different $Sb_4O_5Br_2$/g-C_3N_4-5~90wt%.

FE-SEM-EDS

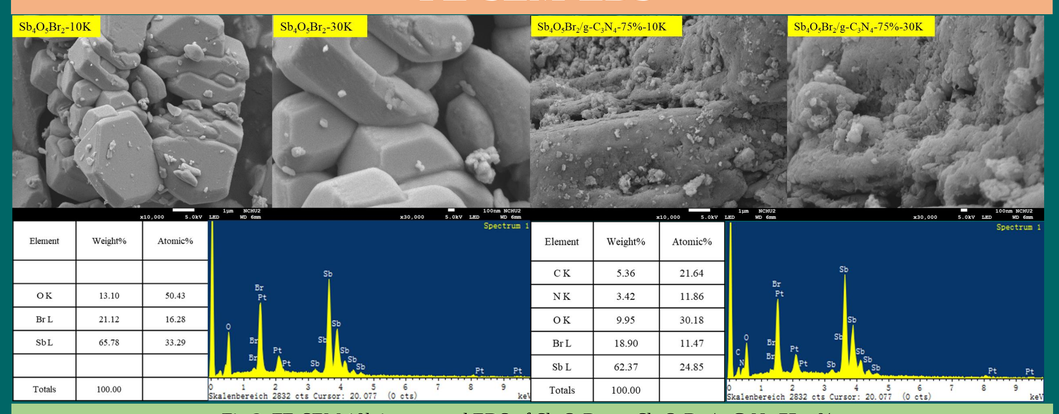

Fig 2. FE-SEM 10k images and EDS of $Sb_4O_5Br_2$ 、 $Sb_4O_5Br_2$/g-C_3N_4-75wt% .

HR-XPS

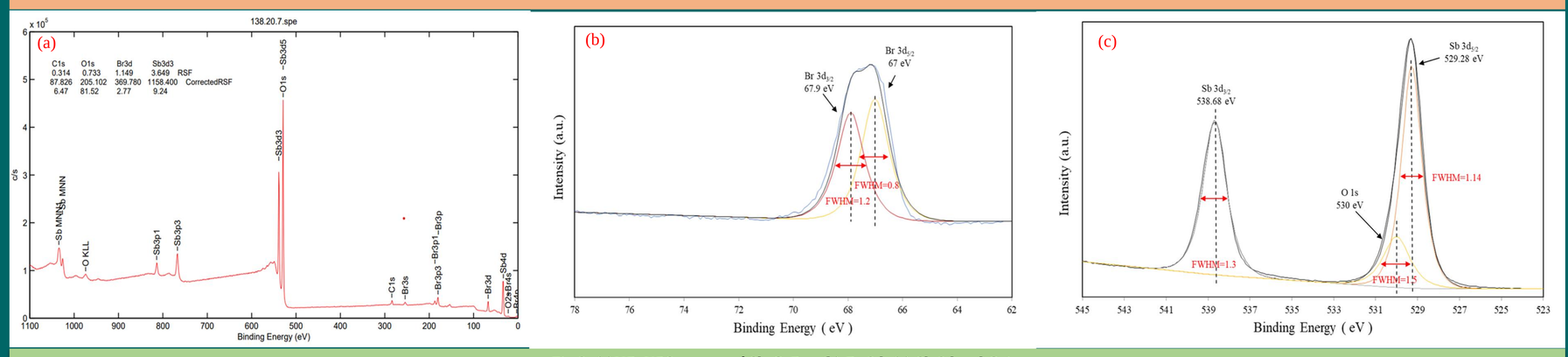

Fig 3. (a)HR-XPS pattern of $Sb_4O_5Br_2$, (b) Br 3d, (c) Sb 3d and O 1s.

UV-DRS

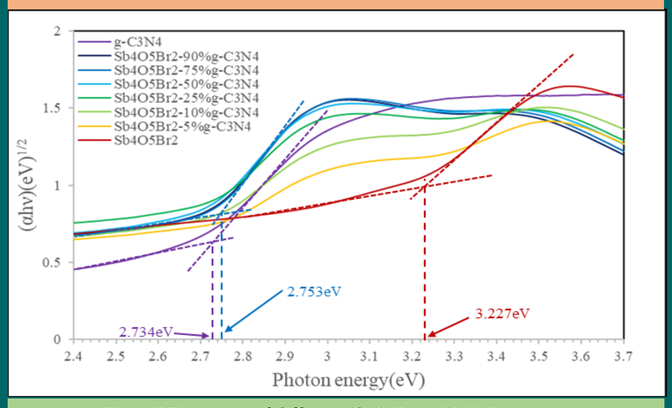

Fig 4. DRS pattern of different $Sb_4O_5Br_2$/g-C_3N_4-5~90wt%.

BET

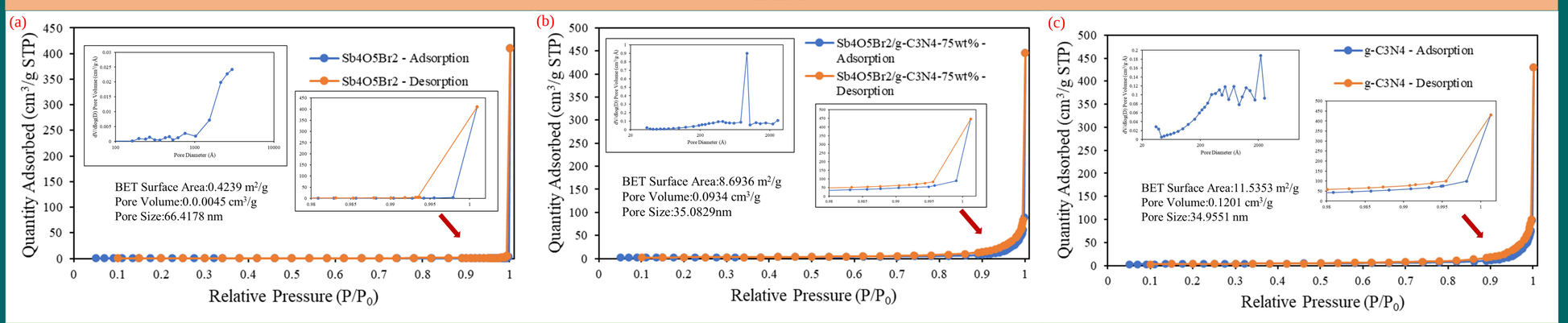

Fig 5. N_2 adsorption isotherm and pore size distribution of (a) $Sb_4O_5Br_2$, (b) $Sb_4O_5Br_2$/g-C_3N_4-75wt%, (c) g-C_3N_4.

PL

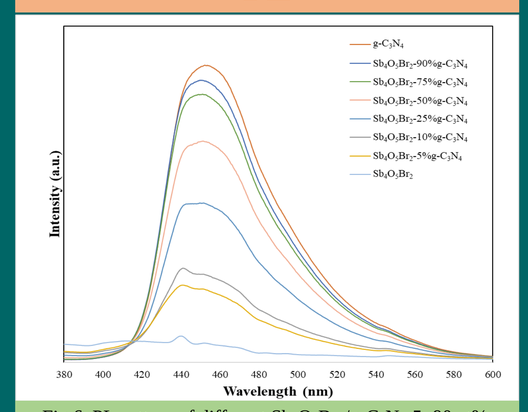

Fig 6. PL pattern of different $Sb_4O_5Br_2$/g-C_3N_4-5~90wt%.

Photocatalytic Degradation of CV

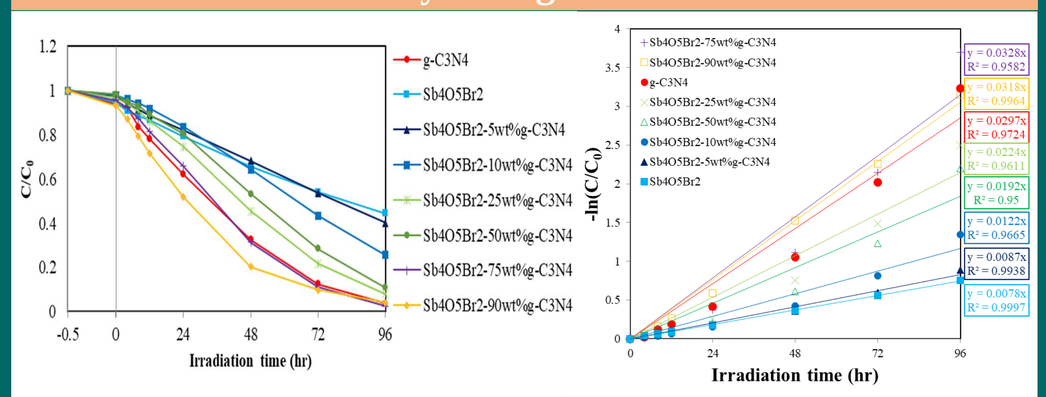

Figure 7. Photodegradation of CV as a function of irradiation time over different $Sb_4O_5Br_2$/g-C_3N_4-5~90wt% photocatalysts.

Photocatalytic Reduction of CO_2

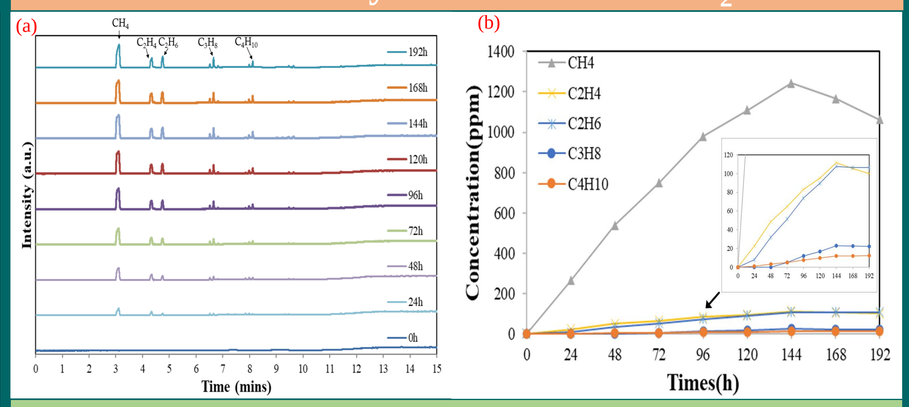

Fig 8. (a) Chromatograph, (b) Photocatalytic reduction of CO_2 by $Sb_4O_5Br_2$.

band structure diagram

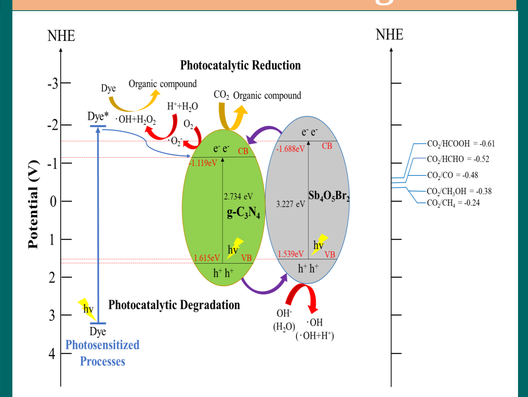

Fig 9. The band structure diagram of Sb4O5Br2/g-C3N4-75wt% photocatalysts.